

Density and Frequency Caudo-Rostral Gradients of Sleep Spindles Recorded in the Human Cortex

Laure Peter-Derex, MD^{1,2,3}; Jean-Christophe Comte, PhD^{2,4}; François Mauguière, MD, PhD^{1,2,5}; Paul A. Salin, MD, PhD^{2,3}

¹Service de Neurologie Fonctionnelle et d'Epileptologie, Hôpital Neurologique, Centre Hospitalier Est, Bron, France; ²Université de Lyon 1, Lyon, France; ³Physiopathologie des réseaux neuronaux du cycle veille-sommeil, INSERM U1028, CNRS UMR 5292, Centre de Recherche en Neurosciences de Lyon, Lyon, France; ⁴CERMEP, Centre Hospitalier Est, Bron, France; ⁵Intégration centrale de la douleur chez l'homme, INSERM U1028, CNRS UMR 5292, Centre de Recherche en Neurosciences de Lyon, Lyon, France

Study Objective: This study aims at providing a quantitative description of intrinsic spindle frequency and density (number of spindles/min) in cortical areas using deep intracerebral recordings in humans.

Patients or Participants: Thirteen patients suffering from pharmaco-resistant focal epilepsy and investigated through deep intracortical EEG in frontal, parietal, temporal, occipital, insular, and limbic cortices including the hippocampus were included.

Methods: Spindle waves were detected from the ongoing EEG during slow wave sleep (SWS) by performing a time-frequency analysis on filtered signals (band-pass filter: 10-16 Hz). Then, spindle intrinsic frequency was determined using a fast Fourier transform, and spindle density (number of spindles per minute) was computed.

Results: Firstly, we showed that sleep spindles were recorded in all explored cortical areas, except temporal neocortex. In particular, we observed the presence of spindles during SWS in areas such as the insular cortex, medial parietal cortex, occipital cortex, and cingulate gyrus. Secondly, we demonstrated that both spindle frequency and density smoothly change along the caudo-rostral axis, from fast frequent posterior spindles to slower and less frequent anterior spindles. Thirdly, we identified the presence of spindle frequency oscillations in the hippocampus and the entorhinal cortex.

Conclusions: Spindling activity is widespread among cortical areas, which argues for the fundamental role of spindles in cortical functions. Mechanisms of caudo-rostral gradient modulation in spindle frequency and density may result from a complex interplay of intrinsic properties and extrinsic modulation of thalamocortical and corticothalamic neurons.

Keywords: Sleep spindles, human, stereo-electro-encephalography, intra-cortical recording, frequency and density analysis

Citation: Peter-Derex L; Comte JC; Mauguière F; Salin PA. Density and frequency caudo-rostral gradients of sleep spindles recorded in the human cortex. *SLEEP* 2012;35(1):69-79.

INTRODUCTION

Spindle waves are a hallmark of stage 2 slow wave sleep in mammals. In human scalp EEG, spindles are grouped in short (0.5 to 3 sec) periods of 11-15 Hz oscillations that occur periodically every 3 to 6 sec and typically appear during the initial stage of slow wave sleep.¹⁻³ The function of sleep spindles has been related to information processing during sleep as they could play a "gating" role, preventing arousal through inhibition of intrusive external stimuli.⁴ Recently, a crucial implication of spindles has been suggested in sleep-dependent memory consolidation.⁵ Indeed, several works in human and rodents have shown that spindle density and spindle power measured in frontal EEG signals are increased during post-learning sleep.⁶

The cognitive roles of sleep spindles could be related to a particular type of information encoding through a high degree of synchrony between the activities of thalamic and cortical neuronal populations during a short time window. Several in vivo and in vitro studies in animals have implicated loops between thalamocortical and thalamic reticular neurons in the generation of spindle

oscillations.⁷⁻⁹ In humans and animals, local field potential recordings have shown that neocortical spindles are phase related to the up state of slow oscillations, and that frontal spindles are closely linked with hippocampal ripples.¹⁰⁻¹² Moreover, unit recordings in the hippocampus and prefrontal cortex during these periods indicate a strong synchronization of spike activity, suggesting that spindles may represent a temporal window for information transfer between the hippocampus and the cortical areas.¹³

In humans, early scalp EEG studies characterized 2 or 3 types of spindles based on the intra-spindle frequency.¹⁴ Since then, authors have converged on the opinion that there are 2 main types of spindles based on the intra-spindle frequency, distinguishing slow (11-13 Hz) from fast (13-15 Hz) spindles.¹⁵⁻¹⁹ Slow spindles are recorded in the frontal areas, while fast spindles are preferentially seen in the centroparietal areas.¹⁶ These results have led to suggest the existence of 2, or even several, spindle generators in human thalamus.¹⁵ Most studies of spindles are based on scalp EEG, which is strongly influenced by the type of reference electrode, sensitive to artifact, and partly blind to signals arising from deep cortical regions such as the inner aspect of the hemispheres and the limbic structures.^{15,16,20} Few studies have been devoted to the description of spindles in deep EEG.^{21,22} Direct recording of the EEG activity through depth electrodes stereotactically implanted in the brain (stereo-electroencephalography or SEEG) is carried out in patients before epilepsy surgery in order to identify the epileptogenic area, the resection of which is expected to result in seizure cessation.²³ This technique allows the recording of neuronal popu-

Submitted for publication February, 2011

Submitted in final revised form August, 2011

Accepted for publication August, 2011

Address correspondence to: Laure Peter-Derex, MD, Service de Neurologie Fonctionnelle et d'Epileptologie, Hôpital Neurologique, Centre Hospitalier Est, 59 Bd Pinel 69677 Bron, France; Tel: (33) 04 72 35 71 68; Fax: (33) 04 72 35 73 97; E-mail: laure.peter@chu-lyon.fr

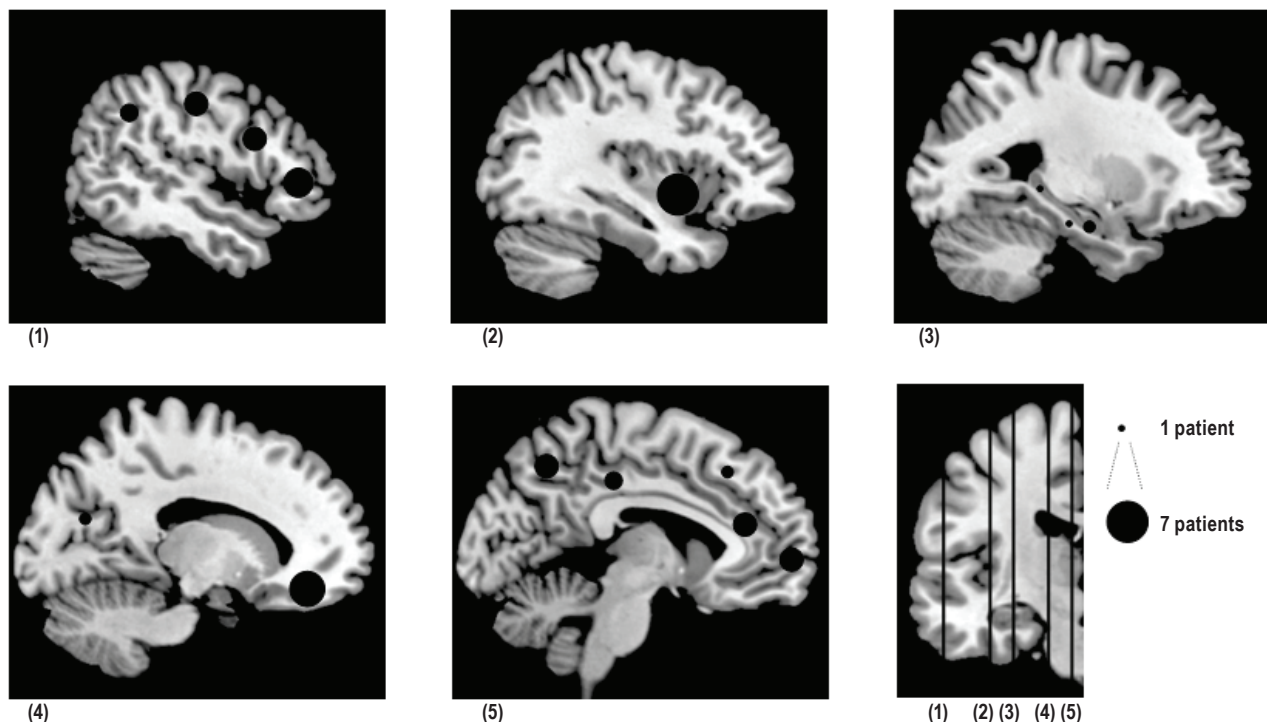


Figure 1—Electrode locations on sagittal T1 MRI slices. Black-filled circles represent electrodes locations on sagittal T1 MRI slices. Topography of the sagittal sections is shown on the bottom right coronal slice, from (1) lateral to (5) medial. For each anatomical location, size is proportional to the number (1 to 7) of the patients explored. **Slice (1)**: posterior lateral frontal cortex (precentral gyrus, precentral sulcus): n = 4; middle lateral frontal cortex (F1 to F3): n = 4; anterior lateral frontal cortex (pole): n = 5; lateral parietal cortex: n = 3. **Slice (2)**: anterior insular cortex: n = 7. **Slice (3)**: anterior hippocampus: n = 2; posterior hippocampus: n = 1; entorhinal cortex: n = 1. **Slice (4)**: orbitofrontal cortex: n = 6; occipital cortex: n = 2. **Slice (5)**: anterior cingulate gyrus: n = 4; posterior cingulate gyrus: n = 3; medial parietal cortex: n = 4; anterior medial frontal cortex: n = 4; middle medial frontal cortex: n = 2.

lation activity in brain regions that are not accessible to scalp EEG. The goal of the present study was to provide a detailed description of spindle frequency and of their regional distribution in the human cortex, including limbic structures.

METHODS

Thirteen patients suffering from pharmaco-resistant focal epilepsy (9 males and 4 females, mean age: 31 years, range: 17-50 years) and investigated with SEEG in the Epilepsy Unit of the Neurological Hospital of Lyon between June 2003 and May 2008 were included in this study. This exploration aimed at identifying the epileptogenic networks in order to propose a surgical curative treatment. The topography of the electrodes implantation was guided by data from noninvasive investigations (clinical history, video-scalp-EEG monitoring, morphologic MRI, and [¹⁸F]-fluorodeoxyglucose position emission tomography). The choice of anatomic targets was different from a patient to another, but the most often explored areas were limbic structures (hippocampus, entorhinal cortex, posterior and anterior cingulate cortex); frontal medial, orbital, and lateral cortex; and in some patients, insular, parietal, or occipital cortex (Figure 1). In 7 patients, the electrode implantation was bilateral. In the present study, the recording sites of interest were selected retrospectively after visual examination of EEG traces and elimination of sites showing interictal spikes and/or nocturnal epileptic discharges.

Intracerebral Stereotactic EEG Procedure

An average of 13 (range: 11-16) depth electrodes per patient were implanted perpendicular to the sagittal plane with a stereotactic frame. Each platinum-iridium electrode had a diameter of 0.8 mm and contained 5 to 15 recording contacts, which were 2 mm long and spaced by 1.5 mm (Dixi, Besançon, France).

The stereotactic implantation procedure was derived from that first described by Talairach and Bancaud (1973) and is detailed in Ostrowsky et al.^{24,25} A cerebral angiogram was first performed in stereotactic conditions using an x-ray source 4.85 m away from the patient's head, to eliminate the linear enlargement due to x-ray divergence. In order to reach the eloquent cortical target, the stereotactic coordinates of each electrode were calculated preoperatively on the individual cerebral MRI previously enlarged at scale 1.²⁶ Cerebral MR and angiographic images were superimposed to avoid any risk of vascular injury during implantation. Electrodes could be left in place chronically up to 15 days. To check the final position of each electrode with respect to the targeted anatomical structures, a post-implantation frontal x-ray was performed and superimposed on MR images.

Video and SEEG signals were collected through bipolar recordings between two neighboring contacts with a sampling rate of 128 Hz (4 patients), 256 Hz (6 patients), or 512 Hz (3 patients) using Micromed software (Treviso, Italy). The high-pass digital filter was set at 0.53 Hz. Value of the low-pass digi-

Table 1—Clinical and demographic characteristics of patients

Patient	Gender/Age	MRI findings	Seizure onset zone	Anti-epileptic drugs (mg/day)	Location of electrodes selected for spindles analysis
1	M/44	Normal	Left temporal pole	Levetiracetam (1000) Gabapentin (800) Lamotrigine (200)	PH, AMFC, ALFC, OFC
2	M/20	Normal	Left parietal cortex	Topiramate (100) Lamotrigine (300)	MMFC, MLFC, PLFC, ACG, OC
3	M/35	Normal	Right lateral temporal cortex	Information not available	MPC, MLFC
4	M/23	Normal	Left basal temporal cortex	Levetiracetam (500) Oxcarbazepine (600)	IC, LPC, MPC, OC
5	M/32	Normal	Right perisylvian cortex	Phenobarbital (150) Carbamazepine (1000) Levetiracetam (1000) Clobazam (15)	AMFC, ALFC, OFC, IC, MPC, ACG
6	F/31	Normal	Right temporal pole	Carbamazepine (200) phenobarbital (150)	IC
7	M/26	Normal	Left amygdala	Oxcarbazepine (1200) Levetiracetam (1000)	AH, OFC, IC, PLFC
8	F/20	Normal	Right amygdala	Levetiracetam (500)	AH, EC, AMFC, ALFC, OFC, PCG, IC, ACG
9	F/50	Normal (lateral temporal cortex dysplasia ?)	Right mesial temporal lobe	Oxcarbazepine (600) Vigabatrin (500)	OFC
10	F/49	Normal	Right temporal pole	Topiramate (400)	AMFC, ALFC, OFC, IC
11	M/17	Normal	Not determined	Clobazam (60)	MLFC, PLFC (x 2), MMFC, ACG
12	M/21	Left occipito-temporal dysplasia	Left occipito-temporal cortex	Valproic acid (500)	LPC, MPC, IC, MLFC, PCG
13	M/33	Lateral frontal cortex dysplasia	Lateral frontal cortex	Carbamazepine (800) Phenytoin (200)	ALFC, PCG, LPC

Abbreviation for location of selected electrodes: AH, anterior hippocampus; PH, posterior hippocampus; EC, entorhinal cortex; ACG, anterior cingulate gyrus; PCG, posterior cingulate gyrus; OFC, orbitofrontal cortex; MFC, medial frontal cortex (AMFC, anteriorMFC; MMFC, middleMFC); LFC, lateral frontal cortex (ALFC, anteriorLFC; MLFC, middleLFC; PLFC, posterior LFC); LPC, lateral parietal cortex; MPC, medial parietal cortex; OC, occipital cortex; IC, insular cortex.

tal filter was fixed at half the values of the different sampling frequencies used, i.e., 64, 128, and 256 Hz. The slope of the filter was 32 dB/octave.

Patients and Epilepsy

All patients were candidates for neurosurgical treatment of partial drug-resistant epilepsy (Table 1). In 10 patients, morphologic brain MRI was normal. Nine patients suffered from temporal lobe epilepsy (TLE), most of them from non-mesial TLE. All patients received anti-epileptic drugs, which were gradually tapered during video-SEEG in order to increase the probability of spontaneous seizures.

All patients were fully informed of the aims and risks of the implantation of SEEG electrodes and of continuous vid-

eo-SEEG monitoring including during sleep; all signed written consents.

Sleep Recording and Scoring

Sleep recordings were carried out approximately 1 week after surgical implantation of electrodes. Recordings started at 21:00-22:00 and continued for about 10 h. EEG, electro-oculogram (EOG), and video recordings were used for sleep scoring. Slow wave sleep (SWS) was identified according to Rechtschaffen and Kales guidelines for 20-sec epochs.¹ The criteria used for sleep states were as follows: for stage 1, presence of theta rhythm; stage 2: presence of spindles and < 20% of delta waves; SWS: > 20% of delta waves; paradoxical sleep: rapid low-voltage EEG resembling wake EEG with rapid eye move-

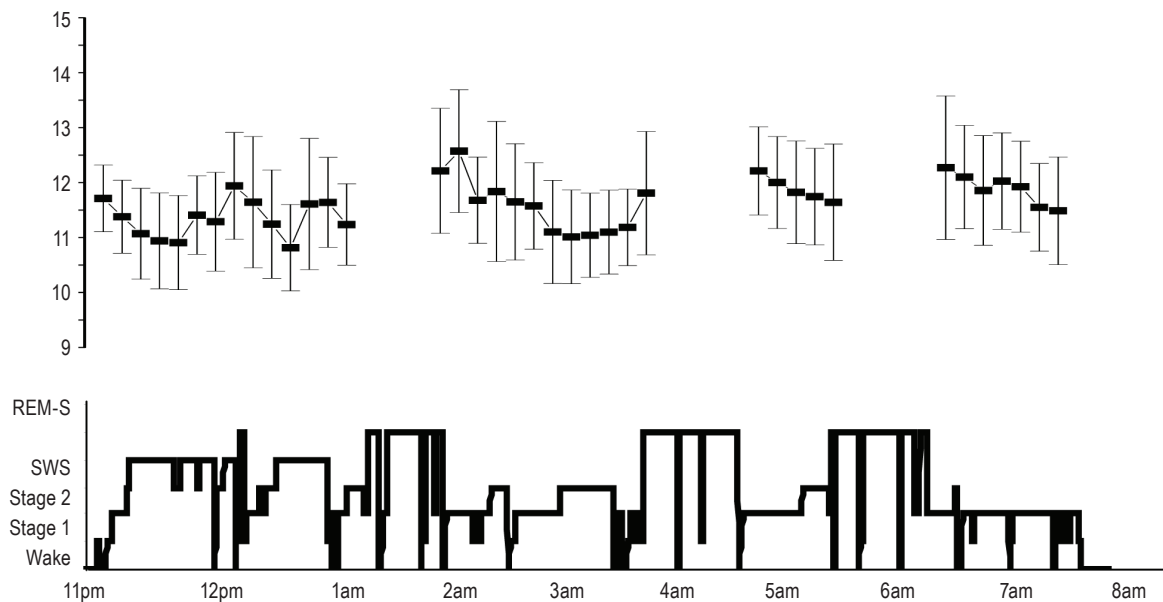


Figure 2—Variation of spindle frequency along nighttime (Typical example from a recording site in the anterior lateral frontal cortex of patient 10). Bottom = Hypnogram. Top: each square represents the mean spindle frequency (\pm SD) during 8-min consecutive NREM sleep periods (for each period, approximately 50 spindles are analyzed). The variation between mean spindle frequency during the first and the fourth period of NREM is significant but weak (11.34 ± 0.24 vs 11.89 ± 0.37 ANOVA, $P < 0.02$). The variations of the mean frequency during the night are situated in the range of the slow spindles (between 10.8 Hz and 12.3 Hz), consistent with the spindle frequency recorded in the lateral frontal cortex.

ment on EOG recordings. In case of doubt between paradoxical sleep and wake, we analyzed the video recordings. Sleep stages were scored by two polysomnographers trained in analyzing intracerebral sleep recordings.

Recording Sites

The EEG traces recorded by bipolar derivation between adjacent contacts were first visually analyzed. For each anatomical region, the trace presenting the best signal-to-noise ratio was selected for further analysis. Following visual analysis, a mean of 4 (1 to 8) sites per patient were selected for spindles study, which were distributed in the following anatomical regions (Figure 1; Table 1):

- *Anterior lateral and medial frontal cortex* ALFC/AMFC (Brodmann area 10-11): 5 and 4 patients, respectively
- *Middle lateral frontal cortex* MLFC (BA 6, 8, 9, 44 to 46): 4 patients
- *Middle medial frontal cortex* MMFC (BA 6, 8, 9, 32): 2 patients
- *Posterior lateral frontal cortex* PLFC (BA 4): 3 patients
- *Orbito-frontal cortex* OFC (BA 12 and 47): 6 patients
- *Anterior cingulate gyrus* ACG (BA 24): 4 patients
- *Posterior cingulate gyrus* PCG (BA 23, 26, 29, and 31): 3 patients
- *Lateral parietal cortex* LPC (BA 7, 39, 40): 3 patients
- *Medial parietal cortex* MPC (BA 7): 4 patients
- *Occipital cortex* OC (BA 18, 19): 2 patients
- *Anterior/posterior Hippocampus* AH/PH (BA 34): 3 patients (11 patients had an hippocampal (5 bilateral) exploration, but for signal analysis, only 3 patients were selected because of the scarcity of epileptic spikes)

- *Entorhinal cortex* EC (BA 28): 1 patient
- *Insular cortex pars anterior and superior* IC (BA 52): 7 patients

Analysis Epochs in SWS Recordings

In 11 patients, we performed our analysis on three 4-min epochs of SWS. During these 12 minutes of SWS we detected an average of 95 ± 32.3 (SD) spindles per site. In 2 patients (Patients 9 and 11), the SWS stage was entirely analyzed during the night in one selected frontal derivation to assess the stability of spindles characteristics throughout the night (Figure 2). In these 2 patients, we observed an increase of ≤ 0.5 Hz in intrinsic spindle frequency from the beginning to the end of the night, indicating that the spindle frequency was quite stable during sleep duration for a given patient. This intra-subject spindle frequency stability has been previously reported in scalp EEG recordings.¹⁶

Signal Analysis

The EEG traces were visually inspected independently by 2 neurologists (LPD and FM), who looked for the presence of spindles and eliminated epochs contaminated by epileptic spikes in the background activity. Then, EEG files were analyzed after conversion using homemade software (<http://www.isc.cnrs.fr/informatique/jcc>). A time-frequency analysis using Morlet wavelets allowed determining the presence (or absence) of pseudo-periodic energy peaks in the 10- to 16-Hz frequency band. To isolate the spindle waves from the ongoing EEG for further analysis, we filtered the signals with a finite impulse response (FIR) band-pass filter: 10-16 Hz. Then, the instantaneous power carried by this frequency band was computed

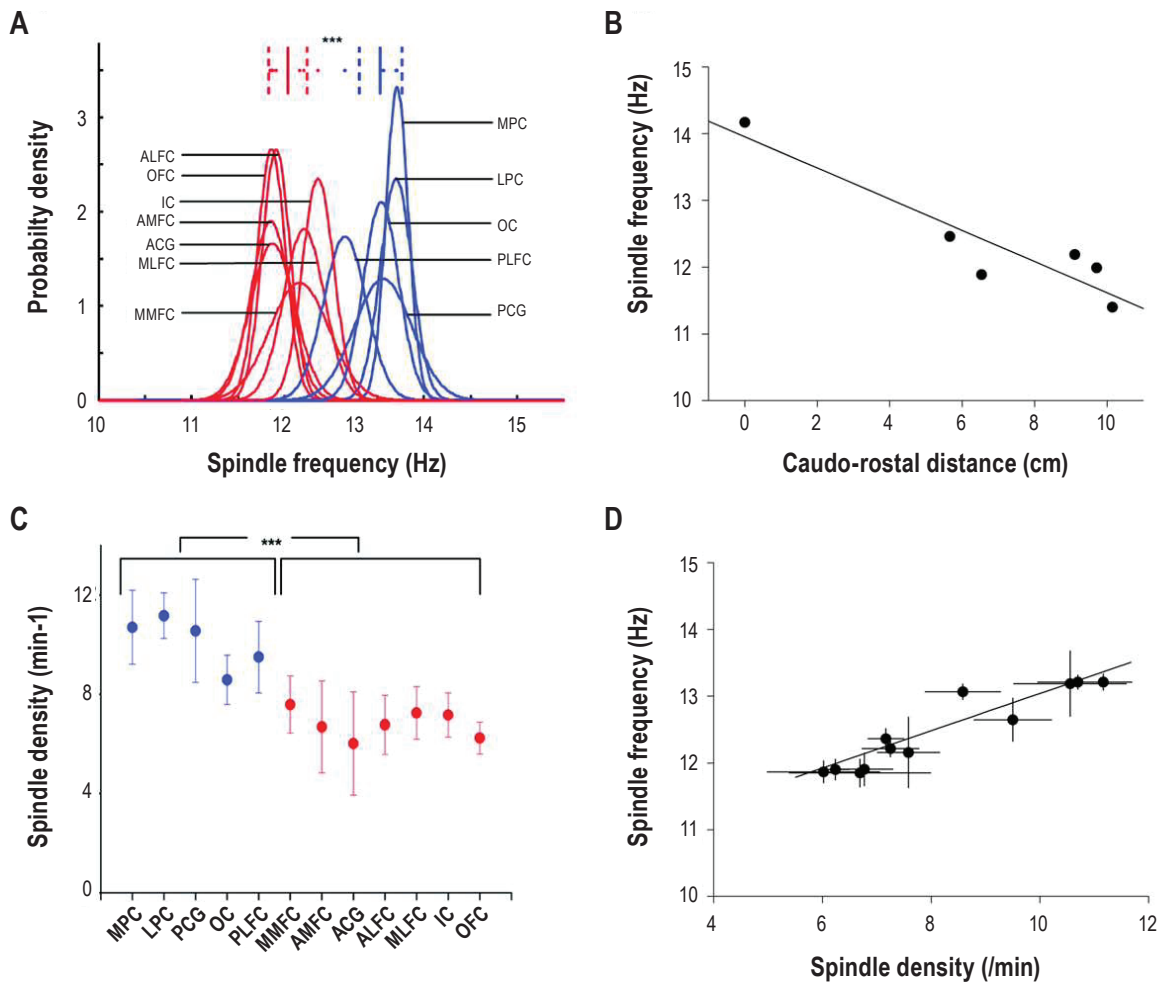


Figure 3—Quantitative analysis of spindle frequency and density. **(A)** Inter-individual comparison of spindles frequency between parieto-occipital and frontal sites. K-means clustering of mean spindle frequency among “fast” (blue) and “slow” (red) sites in pooled patients. Fast spindle sites include parieto-occipital cortex, posterior cingulate gyrus, and posterior lateral frontal cortex. Slow spindle sites include other frontal sites, anterior cingulate gyrus, and anterior insular cortex. The probability density represents the probability to observe a spindle density (/min) for a given frequency in each site. Mean frequency is significantly higher in pooled posterior sites than in pooled anterior sites ($13 \text{ Hz} \pm 0.2 \text{ (SD)}$ vs $12 \text{ Hz} \pm 0.2 \text{ (SD)}$, *t*-test, $P < 0.00005$). **(B)** Linear regression curve between the spindle frequency and the caudo-rostral distance between intermediate sites located in anterior and posterior cingulate gyrus. Unit of the X axis corresponds to the normalized linear distance (cm) from the most caudal recording site in the cingulate gyrus. The spindle frequency is negatively correlated with the linear caudo-rostral distance ($r = -0.99$, $P = 0.007$, $n = 6$). **(C)** Spindle density among different anatomical sites (MPC, medial parietal cortex; LPC, lateral parietal cortex; PCG, posterior cingulate gyrus; OC, occipital cortex; PLFC, posterior lateral frontal cortex; MMFC, middle medial frontal cortex; AMFC, anterior medial frontal cortex; ACG, anterior cingulate gyrus; ALFC, anterior lateral frontal cortex; MLFC, middle lateral frontal cortex; IC, insular cortex; OFC, orbito-frontal cortex). In each site, mean (\pm SD) spindle density in pooled data from recording sites in 12 cortical areas is represented. Spindle density is significantly higher in “fast spindle sites” than in “slow spindle sites” ($10.1/\text{min} \pm 0.7 \text{ (SD)}$ vs $6.8/\text{min} \pm 0.5 \text{ (SD)}$, independent *t*-test, $P < 0.00005$). **(D)** Linear regression curve between spindle frequency and spindle density. Spindle density shows a significant positive correlation with the spindle frequency ($r = 0.94$, $P < 0.0001$) All points are mean from recording sites of the patients for the 12 cortical areas).

using a Gaussian sliding window (1 sec width) applied to the squared signal, and a threshold of 25% was applied to the normalized power magnitude to extract the most significant spindle wave in a given episode. Thus, we computed statistically the spindles of all magnitude scales. Such parameters allowed us to identify spindles with a sensitivity of 85% and a specificity of 95% (in comparison to visual analysis). Once spindles were extracted, the normalized power spectrum (using fast Fourier transform [FFT]) for each spindle was calculated, and the peak of this spectrum F_i (= each spindle intrinsic frequency) determined. Note that in order to reach a 0.1 Hz spectral resolution, we applied the classical zero filling signal processing method

to each detected spindle. This method consists in concatenating null values to the spindle signal in order to extend the signal window size. Since the spectral resolution is proportional to the window size in the time domain, this method allows increasing the resolution without adding information. Finally, we determined the spindle mean frequency (F_m) with previously calculated F_i values and established the frequency distribution of F_i values (number of spindles per frequency band).

In order to classify the frequency of spindles we carried out a k-means clustering algorithm, as shown in Figure 3A. We pre-defined the number of clusters (in our case 2 clusters), and the algorithm partitioned the data (mean spindles frequency in each

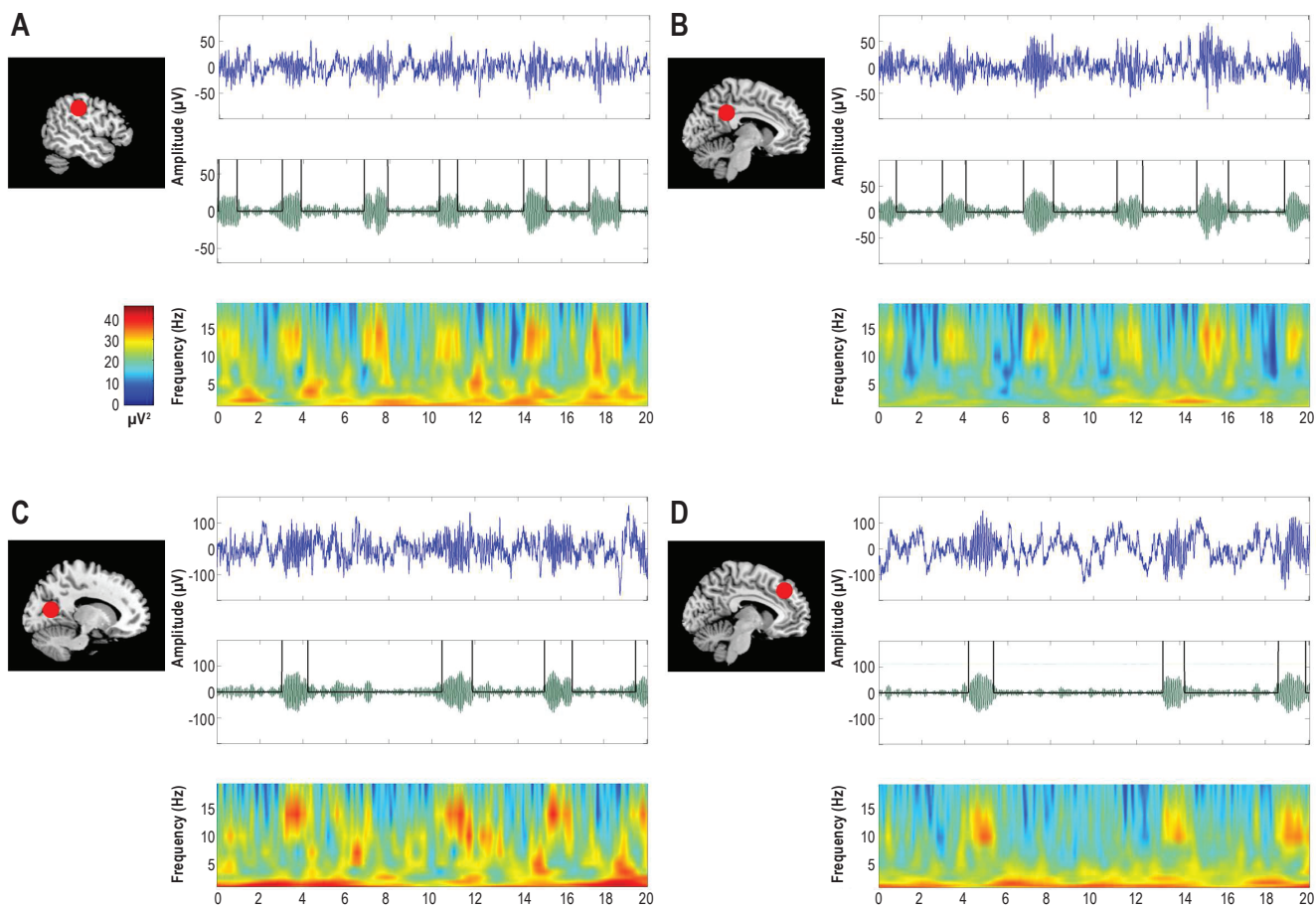


Figure 4—Examples of spindles in selected sites. For each location from top to bottom: (1) Raw EEG trace (20 sec); (2) EEG trace filtered between 10 and 16 Hz for automatic detection; (3) Time-Frequency representation (with color scale for signal power (μV^2)). MRI sagittal slices on the left: red plots indicate the topography of the selected electrode. **A** = lateral parietal cortex (Patient 13); **B** = posterior cingulate gyrus (Patient 12); **C** = occipital cortex (Patient 4); **D** = middle medial frontal cortex (Patient 2).

anatomical site), calculated the mean point, or centroid, of each set and constructed a new partition by associating each point with the closest centroid. Then the centroids were recalculated for the new clusters, and algorithm was iteratively repeated by alternate application of these 2 steps, so that the within-cluster sum of square was minimized.²⁷

Normality of spindle frequency distribution was determined using a Kolmogorov-Smirnov test. All F_i frequency distributions were normal except for middle medial frontal cortex and anterior lateral frontal cortex. Also, means (F_m) and SD of spindle frequency for a given site and for a given patient (and peak F_p of the distribution of F_i values for middle medial frontal cortex and anterior lateral frontal cortex) were used to compare similar sites between subjects and different sites for a given subject, using a t -test. Univariate effect of side, site, and epileptic spikes on spindle frequency in the hippocampus was analyzed with χ^2 test. P values < 0.05 were considered as significant.

RESULTS

Neocortical Spindles

Sleep spindles could be easily detected in SEEG recordings in each neocortical site during SWS (Figure 4). Interestingly,

typical oscillations at spindle frequency were also detected in deep structures, including insular cortex, medial parietal cortex, medial occipital cortex, and cingulate gyrus. In temporal neocortex, sleep spindles were not visually detected and spectral analysis did not show any peak in the 12-14 Hz range. Nevertheless, as many of the patients were suffering from temporal epilepsy, the abundance of epileptic paroxysms in this region prevented us from drawing conclusions.

Frequency analysis of neocortical spindles

Intra-spindle frequency was assessed for all cortical spindles recorded in the different areas. Different peaks in the spindle frequency band emerged from the time-frequency analysis of the EEG signal recorded in different sites. Such topographic differences in intra-spindle frequency were also observed in the Gaussian distribution of each spindle with respect to its intrinsic frequency. Given these results we sought to determine whether the difference in spindle frequency might be observed between frontal and parieto-occipital sites, known from the studies of scalp EEG. Indeed, in patients whose implantation included both frontal and parieto-occipital sites, an antero-posterior gradient in the distribution of spindle frequency was observed: spindles recorded in fron-

Table 2—Intra-individual differences in spindle frequency among sites

Patient	Anterior sites		Posterior sites		t-test
	Location	Mean spindles frequency (Hz) ± SD	Location	Mean spindles frequency (Hz) ± SD	
2	MMFC+MLFC+PLFC+ ACG	11.8 ± 0.4	OC	13 ± 0.1	P < 0.0005
3	MLFC	12.2 ± 0.3	MPC	13.4 ± 0.1	P < 0.005
5	AMFC+ALFC+OFC	11.5 ± 0.1	OC	13.3 ± 0.3	P < 0.005
12	MLFC	11.9 ± 0.2	MPC+LPC	13 ± 0.4	P < 0.00005
13	ALFC	11.3 ± 0.1	LPC	13.2 ± 0.3	P < 0.005

In each of the 5 patients recorded in both anterior and posterior sites, spindle frequency was significantly higher in pooled parieto-occipital sites than in between pooled frontal sites. Abbreviations for locations are the same as in Table 1

tal sites were significantly slower than spindles recorded in parieto-occipital sites (Table 2).

We used the k-means clustering algorithm (see Methods) to classify spindles according to their intrinsic frequency. Several anterior sites (AMFC, ALFC, OFC, and ACG) showed slow spindles, whereas parieto-occipital sites (LPC, MPC, and PCG) exhibited fast spindles ($P < 0.0005$). However, although 2 clusters of slow and fast spindles emerged from this analysis, clear intermediate spindle frequencies were also observed in 4 different recording sites (MMFC, MLFC, IC, and PLFC, Figure 3A). To determine whether these differences in spindle frequency correspond to a caudo-rostral gradient or to distinct spindle frequencies in frontal and parieto-occipital areas, we correlated in the cingulate gyrus (where recording sites are in the same sagittal plane) the spindle frequency with the rostrocaudal position of each electrode (Figure 3B). Although the number of sites was small, the linear regression between the caudo-rostral position of recording site and the spindle frequency was significant ($r = -0.99$, $P = 0.007$, $n = 6$, Figure 3B). This observation suggests that the differences in spindle frequency between parieto-occipital and frontal sites might result from a progressive caudo-rostral change in spindle frequency and not from a steep separation between frontal and parieto-occipital areas.

Density analysis of neocortical spindles

Next, we examined the spindle density (number of spindles/min). We observed that in neocortical sites with fast spindles, the spindle density was 50% higher than in sites with slow spindles ($10.1 \pm 0.2/\text{min}$ vs $6.8 \pm 0.2/\text{min}$, $P < 0.0001$; Figure 3C). As for the intra-spindle frequency, spindles recorded in some sites (MMFC, PLFC) represented intermediate values of spindle density between frontal and parieto-occipital areas. This prompted us to determine whether there was a correlation between spindle density and intra-spindle frequency when data from all neocortical sites were pooled together. Indeed we found a highly significant positive correlation between the spindle density and frequency ($r = 0.94$, $P < 0.0001$, Figure 3D). Altogether, our results suggest a gradient of spindle frequency and density along the caudo-rostral axis.

Spindle frequency oscillations in the hippocampus and entorhinal cortex during SWS

In the hippocampus, oscillatory bursts around 14 Hz sharing the typical features of neocortical sleep spindles were observed

in 7 hippocampi (7 patients), while in the remaining 8 patients, epileptic spikes prevented us from carrying out an analysis of hippocampal oscillations. In 5 patients the hippocampal implantation was bilateral, and in 3 patients both the anterior and the posterior hippocampus were explored. In patients with bilateral exploration, hippocampal spindle frequency oscillation (HSO) emerged unilaterally in 4 patients, ipsilateral to the epileptogenic focus in 2 cases and contralateral in the 2 others. We analyzed the effect of the side (ipsilateral to the epileptic focus vs contralateral), the site (anterior vs posterior hippocampus), and the presence or the absence of spikes: none of these variables was predictive for absence or presence of HSO (Figure 5A). Nevertheless, in the only hippocampus without any epileptic spikes at the time of the recording, sleep spindles were clearly observed (Figure 5B, Patient 8). In 2 patients (Patients 7 and 8) with no or very rare epileptic spikes in the anterior hippocampus, the mean HSO frequency was 13.4 ± 0.5 Hz and the HSO density was $5.4 \pm 4.3/\text{min}$. In patient 1, with rare epileptic spikes in the posterior hippocampus, the mean HSO frequency was 13.4 ± 0.5 Hz and the HSO density was $11.3 \pm 3.5/\text{min}$. In contrast, Figure 5B illustrates an example of recordings in a patient with rich epileptic spiking activity. In this case, no HSO was observed during the whole recorded period (Figure 4B, Patient 5). Interestingly also, Patient 8, without any epileptic spikes in the hippocampus, had electrodes in the entorhinal cortex, an area strongly interconnected with the dentate gyrus, the hippocampus proper and the subiculum. The entorhinal cortex activity recorded in this patient exhibited spindle frequency oscillations, with a mean frequency of 14.2 ± 0.6 and a density of $5.3 \pm 0.5/\text{min}$, similar to those observed in the hippocampus. These results suggest that mesiotemporal limbic structures exhibit spindle oscillations whose frequency is close to that of fast cortical spindles.

DISCUSSION

In the present study, we first showed that sleep spindles were generated in all recorded cortical areas, except temporal neocortex where the abundance of epileptic paroxysms prevented us from drawing conclusions (one can note that Nakabayashi et al., did not find any spindles in medial and basal temporal lobe with electrocorticographic recordings).²⁸ In particular, we observed the presence of spindles during SWS in areas such as insular cortex, medial parietal cortex, occipital cortex, and cingulate gyrus. Second, we demonstrated that

		Ipsilateral hippocampus		Contralateral hippocampus	
		Anterior hippocampus	Posterior hippocampus	Anterior hippocampus	Posterior hippocampus
SPIKES +	HSO +	2	2	2	0
	HSO -	8	1	2	1
SPIKES -	HSO +	1	0	0	0
	HSO -	0	0	0	0

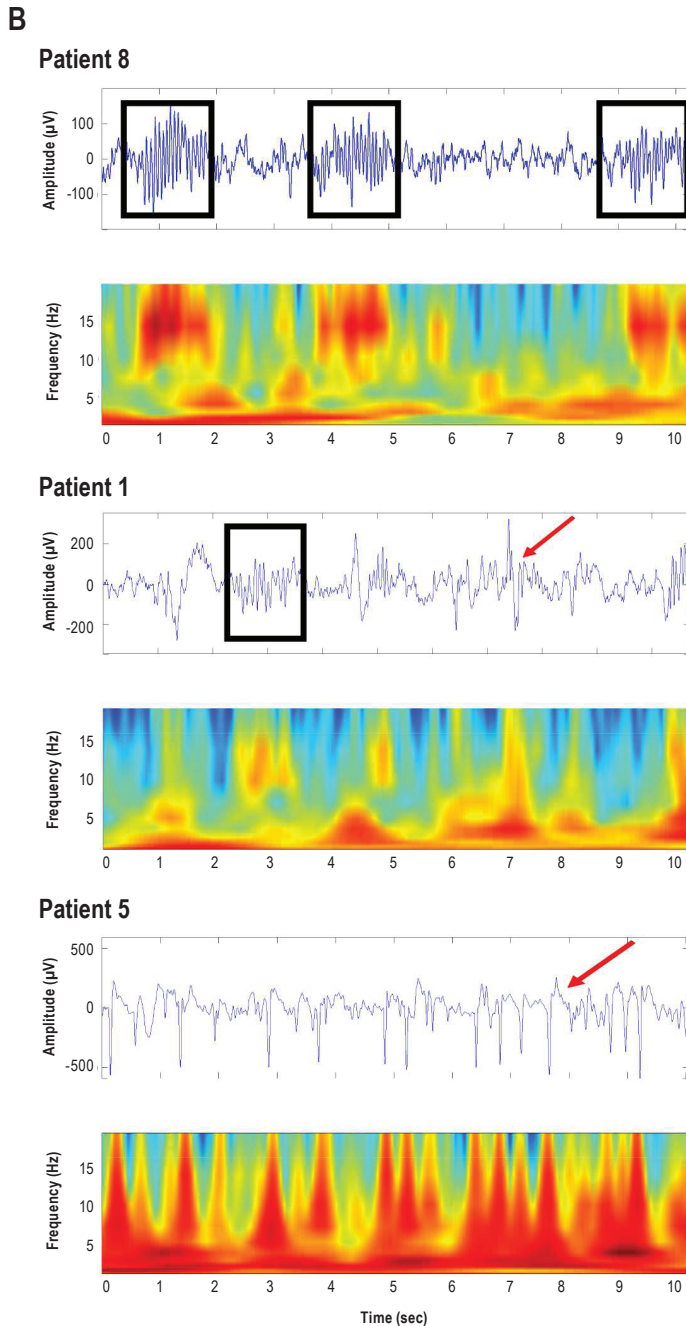


Figure 5—Hippocampal spindle frequency oscillations (HSO). The table shows the distribution (number of patients) of HSO according to the presence of spikes and the location. No significant correlation was found for presence vs absence of HSO according to the side (ipsilateral to the epileptic focus vs contralateral), the site (anterior vs posterior hippocampus), and the presence or the absence of spikes (χ^2 , $P > 0.3$, $n = 21$). Examples of hippocampus EEG traces and time-frequency analysis (10 sec) during SWS sleep (spikes = red arrow, spindles = black squares). Top: no spikes and HSO (Patient 8); Middle: spikes and HSO (Patient 1); Bottom: spikes and no HSO (Patient 5).

both spindle frequency and density change smoothly along the caudo-rostral axis. Finally, we identified the presence of spindle frequency oscillations in the hippocampus and the entorhinal cortex.

Before discussing the results, we have first to address some methodological issues. Results were obtained in epileptic patients in whom cross-interferences may occur between sleep oscillations and epileptogenic mechanisms.²⁹ In epileptic neurons of mesial temporal lobe, higher firing rates and increased synchronous firing have been observed during SWS and paradoxical sleep compared with wakefulness.³⁰ At a macroscopic level, the activation of interictal epileptic discharges by sleep spindles is well known.³¹ Enhanced spindle activity has been described in the epileptic hemisphere in patients suffering from partial epilepsy.³² Nevertheless, the spindle characteristics we observed in our study did not differ from those reported in scalp EEG studies of non-epileptic subjects. Moreover, as indicated in Methods, two neurologists (co-authors of the present article) discarded independently the recordings showing interictal spiking activity. The antiepileptic medications taken by the patients can also interfere with electrogenesis, but most of these treatments are only known to modulate spindle density.³³ Lastly, all patients included in this study suffer from focal epilepsy and are candidates to a surgical curative treatment. This implies that after successful resection of the “epileptic focus” the brain of these patients will return to a non-epileptic, or rather a non-epileptogenic, status. The situation would have been quite different in the context of idiopathic generalized epilepsy, where epileptogenesis (which is likely to be genetically determined in this type of epilepsy) represents a characteristic supposed to be common to all, or most of, thalamocortical circuits.³⁴ Thus, although we are unable to bring evidence that epileptic and non-epileptic brains generate spindles in a similar fashion, spindles recorded in the non-epileptogenic cortical areas of our patients look usable for approaching sleep spindle physiology.

Another issue concerns the new methods of signal analysis we developed. Automatic detection of spindles could misclassify some oscillations as spindles. However, the reliability of the software detection of spindles was counterchecked by a careful visual examination of the oscillations. We chose selective automatic detection criteria in order to reach a high detection specificity (approximately 95%), to the detriment of the detection sensitivity, which was, however, 85%. This procedure entailed the risk of spindle density underestimation. Nevertheless, this slight decrease in detection sensibility probably did not introduce any bias in the quantification of the fast/slow spindle density ratio, which was similar to that reported in scalp EEG studies.²⁰

To our knowledge, the present study is the first in which sleep spindle density and frequency have been studied in relation to their topography using intra-cortical electrodes in the human brain. Nakumara et al., using electrocorticographic surface recordings, have shown that low-frequency spindle oscillations around 12 Hz were widely distributed across orbital, medial, dorsolateral prefrontal cortices and frontal pole.²¹ These authors reported that spindle frequency peak value in frontal sites was slower than that observed at the midline central site [Cz] (13.5 Hz), but no postcentral deep recording sites were available in their study. We observed similar results in prefrontal sites and added information about posterior fast spindles. These results confirm scalp EEG and magnetoencephalographic studies, which described two or three types of spindles.^{14,15,20,35} Differences between spindles not only concern frequency and density but also homeostatic and circadian regulation, as well as pharmacologic and hormonal modulation or maturation during life.^{3,16,36-39} Moreover, learning-dependent increase in spindle density has shown local specificity, depending on the type of the pre-sleep learning task. Verbal memory retention has been positively correlated to an increase in the low-frequency sleep spindle density in left frontocentral areas, motor-skills tasks with spindle activity in contralateral central area, and spatial visuomotor task with fast-spindle activity in parietal areas.⁴⁰⁻⁴³

What could be the mechanism generating differences in spindle frequencies? It has been shown that spindle bursting oscillations emerge from reciprocal interactions between GABA-ergic inhibitory nucleus reticularis thalamic neurons and excitatory thalamocortical relay neurons.⁴⁴ The reticular thalamic nucleus acts as a pacemaker, which induces rhythmic hyperpolarization and consecutive rebound depolarization secondary to low threshold calcium spike activation in thalamocortical neurons. Thalamocortical neurons connect to neurons in different cortical areas giving rise to the spindle waves.⁴⁵ A change in ion channel conductance of thalamocortical neurons projecting on frontal and parieto-occipital cortex may thus explain spindle frequency differences between these two cortical regions.⁸ Slow and fast spindles could thus emerge from distinct thalamocortical networks involving, respectively, the reticular nucleus, mediodorsal and anterior thalamic nuclei, prefrontal, orbito-frontal, anterior insular, and anterior cingulate cortices for slow cortical spindle oscillations, and the reticular nucleus, ventral lateral, and posterior thalamic nuclei including pulvinar, precentral, postcentral, parietal, occipital, and temporal cortices for fast posterior spindles.⁴⁶⁻⁴⁸ However, our results are not in favor of an abrupt change in spindle frequency between anterior and posterior recording sites, but rather show a progres-

sive rostro-caudal modulation in spindle frequency and density. This finding suggests that cortico-cortical and cortico-thalamic connections could modulate the spindling activity generated by reticulo-thalamic and thalamocortical neurons. This hypothesis is supported by several studies in animals showing an important role of cortico-thalamic connections in sleep spindle generation.^{49,50} The recent study of Nir et al. also argues for local modulation of thalamocortical activity in SWS.²² Finally, the study of Debay et al. suggests an influence of peripheral sensory inputs on spindle density, which increases when the synaptic bombardment of thalamocortical neurons by retinal ganglion cells decreases.⁵¹ Thus the caudo-rostral modulation of spindle density and frequency may result from a complex interplay of intrinsic properties and extrinsic modulation of thalamocortical and corticothalamic neurons.

We observed spindle frequency oscillations in the hippocampus, ipsilateral or contralateral to the epileptic focus, in both the epileptic and non-epileptic hippocampus. This result confirms and further underlines the physiological role of such oscillations in the hippocampus. Oscillation of 12 to 14 Hz have been recorded in the hippocampus by several authors.^{53,54} These articles suggested that such oscillations were either a physiological activity or an evoked response of the hippocampus to an epileptic afferent discharge. In other studies, "limbic spindles" have been found to occur simultaneously or independently of surface spindles, without any relationship with the epileptogenic region.⁵⁴⁻⁵⁶ In monkeys, the posterior parahippocampal gyrus is connected, as the posterior cingulate gyrus, to the medial nucleus of the pulvinar but also to the so-called limbic nuclei (anterior nuclear group and laterodorsal nucleus), and to the lateral-posterior nucleus, which is modality-specific.^{58,59} In rats and cats, the hippocampal formation (including CA1, the entorhinal cortex, and the subiculum) are connected to the anterior thalamus, in particular to the nucleus reuniens, and in squirrel monkeys to anterior and laterodorsal thalamic nuclei.⁵⁹⁻⁶¹ Thus sleep spindles may emerge from mesial temporal areas, as these structures receive connections from thalamic nuclei.⁶² The question whether they result from thalamo-hippocampal loops is important, given the role of thalamo-hippocampal circuits in learning and memory.⁶³

In summary, we recorded sleep spindles from almost every cortical area that was explored with deep electrodes. This argues for the fundamental role of spindles in cortical functions. Mechanisms of caudo-rostral gradient modulation in spindle frequency and density remain hypothetical and would require further studies based on simultaneous recordings of thalamic and neocortical spindles. However, our study does not fit with the concept of two distinct thalamocortical circuitries generating anterior slow and posterior fast spindles, and rather suggest a continuous rostrocaudal change of spindle frequencies reflecting the existence of multiple thalamocortical circuits and their modulation by corticothalamic and cortico-cortical connections.

ACKNOWLEDGMENTS

The authors thank Marc Guénot for stereotactic electrodes implantations, Hélène Bastuji for collaboration in sleep recordings analysis, and Michel Magnin for constructive input and critical reading of the manuscript. This study was performed at the Hôpital Neurologique, Centre Hospitalier Est, 59 Bd Pinel 69677 Bron, France.

DISCLOSURE STATEMENT

This was not an industry supported study. The authors have indicated no financial conflicts of interest.

REFERENCES

1. Rechtschaffen A, Kales R (eds). A manual of standardized terminology, techniques and scoring system for sleep stage of human subjects. Washington, DC: Public Health Service, US Government Printing Office, 1968.
2. De Gennaro L, Ferrara M. Sleep spindles: an overview. *Sleep Med Rev* 2003;7:423-40.
3. Nicolas A, Petit D, Rompré S, Montplaisir J. Sleep spindle characteristics in healthy subjects of different age groups. *Clin Neurophysiol* 2001;112:521-7.
4. Steriade M, Llinás RR. The functional states of the thalamus and the associated neuronal interplay. *Physiol Rev* 1988;68:649-742.
5. Gais S, Mölle M, Helms K, Born J. Learning-dependent increases in sleep spindle density. *J Neurosci* 2002;22:6830-4.
6. Clemens Z, Fabó D, Halász P. Overnight verbal memory retention correlates with the number of sleep spindles. *Neuroscience* 2005;132:529-35.
7. Morison RS, Bassett DL. Electrical activity of the thalamus and basal ganglia in decorticate cats. *J Neurophysiol* 1945;8:309-14.
8. Steriade M, Domich L, Oakson G, Deschênes M. The deafferented reticular thalamic nucleus generates spindle rhythmicity. *J Neurophysiol* 1987;57:260-73.
9. McCormick DA, Bal T. Sleep and arousal: thalamocortical mechanisms. *Annu Rev Neurosci* 1997;20:185-215.
10. Steriade M, Nuñez A, Amzica F. Intracellular analysis of relations between the slow (< 1 Hz) neocortical oscillation and other sleep rhythms of the electroencephalogram. *J Neurosci* 1993;13:3266-83.
11. Clemens Z, Mölle M, Eross L, Barsi P, Halász P, Born J. Temporal coupling of parahippocampal ripples, sleep spindles and slow oscillations in humans. *Brain* 2007;130:2868-78.
12. Clemens Z, Mölle M, Eröss L, et al. Born J. Fine-tuned coupling between human parahippocampal ripples and sleep spindles. *Eur J Neurosci* 2010;33:511-20.
13. Wierzynski CM, Lubenov EV, Gu M, Siapas AG. State-dependent spike-timing relationships between hippocampal and prefrontal circuits during sleep. *Neuron* 2009;61:587-96.
14. Gibbs FA, Gibbs EL. Atlas of electroencephalography. Vol 1. Cambridge MA: Addison-Wesley, 1950.
15. Jobert M, Poiseau E, Jähnig P, Schulz H, Kubicki S. Topographical analysis of sleep spindle activity. *Neuropsychobiology* 1992;26:210-7.
16. Werth E, Achermann P, Dijk DJ, Borbély AA. Spindle frequency activity in the sleep EEG: individual differences and topographic distribution. *Electroencephalogr Clin Neurophysiol* 1997;103:535-42.
17. Zygierevicz J, Blinowska KJ, Durka PJ, Szelenberger W, Niemcewicz S, Androsiuk W. High resolution study of sleep spindles. *Clin Neurophysiol* 1999;110:2136-47.
18. Anderer G, Klosch G, Gruber G, et al. Low-resolution brain electromagnetic tomography revealed simultaneously active frontal and parietal sleep spindle sources in the human cortex. *Neuroscience* 2001;103:581-92.
19. Schabus M, Dang-Vu TT, Albouy G, et al. Hemodynamic cerebral correlates of sleep spindles during human non-rapid eye movement sleep. *PNAS* 2007;104:13164-69.
20. Zeitlhofer J, Gruber G, Anderer P, Asenbaum S, Schimicek P, Saletu B. Topographic distribution of sleep spindles in young healthy subjects. *J Sleep Res* 1997;6:149-55.
21. Nakamura M, Uchida S, Maehara T, et al. Sleep spindles in human prefrontal cortex: an electrocorticographic study. *Neurosci Res* 2003;45:419-27.
22. Nir Y, Staba RJ, Andrillon T, et al. Regional slow waves and spindles in human sleep. *Neuron* 2011;70:153-69.
23. Guenot M, Isnard J, Ryvlin P, et al. Neurophysiological monitoring for epilepsy surgery: the Talairach SEEG method. *StereoElectroEncephalography*. Indications, results, complications and therapeutic applications in a series of 100 consecutive cases. *Stereotact Funct Neurosurg* 2001;77:29-32.
24. Bancaud J, Talairach J. Methodology of stereo EEG exploration and surgical intervention in epilepsy. *Rev Otoneuroophthalmol* 1973;4:315-28.
25. Ostrowsky K, Magnin M, Ryvlin P, Isnard J, Guenot M, Mauguère F. Representation of pain and somatic sensation in the human insula: a study of responses to direct electrical cortical stimulation. *Cereb Cortex* 2002;12:376-85.
26. Talairach J, Tournoux P. Co-planar stereotaxic atlas of the human brain. Stuttgart: Thieme, 1988.
27. Hartigan JA. Clustering algorithms. New York: John Wiley & Sons, 1975.
28. Nakabayashi T, Uchida S, Maehara T, et al. Absence of sleep spindles in human medial and basal temporal lobes. *Psychiatry Clin Neurosci* 2001;55:57-65.
29. Steriade M, Amzica F. Sleep oscillations developing into seizures in corticothalamic systems. *Epilepsia* 2003;44:9-20.
30. Staba RJ, Wilson CL, Bragin A, Fried I, Engel J Jr. Sleep states differentiate single neuron activity recorded from human epileptic hippocampus, entorhinal cortex, and subiculum. *J Neurosci* 2002;22:5694-704.
31. Nobili L, Ferrillo F, Baglietto MG, et al. Relationship of sleep interictal epileptiform discharges to sigma activity (12-16 Hz) in benign epilepsy of childhood with rolandic spikes. *Clin Neurophysiol* 1999;110:39-46.
32. Clemens B, Ménes A. Sleep spindle asymmetry in epileptic patients. *Clin Neurophysiol* 2000;111:2155-9.
33. Hirshkowitz M, Thornby JJ, Karacan I. Sleep spindles: pharmacological effects in humans. *Sleep* 1982;5:85-94.
34. Steriade M. Sleep, epilepsy and thalamic reticular inhibitory neurons. *Trends Neurosci* 2005;28:317-24.
35. Urakami Y. Relationships between sleep spindles and activities of cerebral cortex as determined by simultaneous EEG and MEG recording. *J Clin Neurophysiol* 2008;25:13-24.
36. Brunner DP, Münch M, Biedermann K, Huch R, Huch A, Borbély AA. Changes in sleep and sleep electroencephalogram during pregnancy. *Sleep* 1994;17:576-82.
37. Aeschbach D, Dijk DJ, Trachsel L, Brunner DP, Borbély AA. Dynamics of slow-wave activity and spindle frequency activity in the human sleep EEG: effect of midazolam and zopiclone. *Neuropsychopharmacology* 1994;11:237-44.
38. Aeschbach D, Dijk DJ, Borbély AA. Dynamics of EEG spindle frequency activity during extended sleep in humans: relationship to slow-wave activity and time of day. *Brain Res* 1997;748:131-6.
39. Driver HS, Dijk DJ, Werth E, Biedermann K, Borbély AA. Sleep and the sleep electroencephalogram across the menstrual cycle in young healthy women. *J Clin Endocrinol Metab* 1996;81:728-35.
40. Clemens Z, Fabó D, Halász P. Overnight verbal memory retention correlates with the number of sleep spindles. *Neuroscience* 2005;132:529-35.
41. Schmidt C, Peigneux P, Muto V, et al. Encoding difficulty promotes postlearning changes in sleep spindle activity during napping. *J Neurosci* 2006;26:8976-82.
42. Barakat M, Doyon J, Debas K, et al. Fast and slow spindle involvement in the consolidation of a new motor sequence. *Behav Brain Res* 2011;217:117-21.
43. Tamaki M, Matsuoka T, Nittono H, Hori T. Fast sleep spindle (13-15 Hz) activity correlates with sleep-dependent improvement in visuomotor performance. *Sleep* 2008;31:204-11.
44. Steriade M, McCormick DA, Sejnowski TJ. Thalamocortical oscillations in the sleeping and aroused brain. *Science* 1993;262:679-85.
45. Steriade M. The corticothalamic system in sleep. *Front Biosci* 2003;8:878-99.
46. Van Buren JM, Burke RC. Variation and connection of the human thalamus. 1. the nuclei and cerebral connections of the human thalamus. New York: Springer-Verlag, 1972.
47. Guillery RW, Harting JK. Structure and connections of the thalamic reticular nucleus: Advancing views over half a century. *J Comp Neurol* 2003;463:360-71.
48. Behrens TE, Johansen-Berg H, Woolrich MW, et al. Non-invasive mapping of connections between human thalamus and cortex using diffusion imaging. *Nat Neurosci* 2003;6:750-7.
49. Steriade M, Wyzinski P, Apostol V. Corticofugal projections governing rhythmic thalamic activity. In Frigyesi TL, Rinvik E, Yahr MD, eds. *Corticothalamic projections and sensorimotor activities*. New York: Raven, 1972:221-72.
50. Bal T, Debay D, Destexhe A. Cortical feedback controls the frequency and synchrony of oscillations in the visual thalamus. *J Neurosci* 2000;20:7478-88.
51. Debay D, Wolfart J, Le Franc Y, Le Masson G, Bal T. Exploring spike transfer through the thalamus using hybrid artificial-biological neuronal networks. *J Physiol Paris* 2004;98:540-58.
52. Brazier M. Interactions of deep structures during seizures in man. In: Petsche U, Brazier M, eds. *Mechanisms of synchronization in epileptic seizures*. Vienna: Springer, 1972: 409.

53. Montplaisir J, Leduc L, Laverdière M, Walsh J, Saint-Hilaire JM. Sleep spindles in the human hippocampus: normal or epileptic activity? *Sleep* 1981;4:423-8.
54. Wieser HG. Temporal lobe epilepsy, sleep and arousal: stereo-EEG findings. *Epilepsy Res Suppl* 1991;2:97-119.
55. Malow BA, Carney PR, Kushwaha R, Bowes RJ. Hippocampal sleep spindles revisited: physiologic or epileptic activity? *Clin Neurophysiol* 1999;110:687-93.
56. Asano E, Mihaylova T, Juhász C, Sood S, Chugani HT. Effect of sleep on interictal spikes and distribution of sleep spindles on electrocorticography in children with focal epilepsy. *Clin Neurophysiol* 2007;118:1360-8.
57. Baleyrier C, Mauguier F. Anatomical evidence for medial pulvinar connections with the posterior cingulate cortex, the retrosplenial area, and the posterior parahippocampal gyrus in monkeys. *J Comp Neurol* 1985;232:219-28.
58. Yeterian EH, Pandya DN. Corticothalamic connections of paralimbic regions in the rhesus monkey. *J Comp Neurol* 1988;269:130-46.
59. DeVito JL. Subcortical projections to the hippocampal formation in squirrel monkey (*Saimira sciureus*). *Brain Res Bull* 1980;5:285-9.
60. Yanagihara M, Ono K, Niimi K. Thalamic projections to the hippocampal formation in the cat. *Neurosci Lett* 1985;61:31-5.
61. Dolleman-Van Der Weel MJ, Witter MP. Projections from the nucleus reuniens thalami to the entorhinal cortex, hippocampal field CA1, and the subiculum in the rat arise from different populations of neurons. *J Comp Neurol* 1996;364:637-50.
62. Cavdar S, Onat FY, Cakmak YO, Yananli HR, Gülçebi M, Aker R. The pathways connecting the hippocampal formation, the thalamic reuniens nucleus and the thalamic reticular nucleus in the rat. *J Anat* 2008;212:249-56.
63. Aggleton JP, Poirier GL, Aggleton HS, Vann SD, Pearce JM. Lesions of the fornix and anterior thalamic nuclei dissociate different aspects of hippocampal-dependent spatial learning: implications for the neural basis of scene learning. *Behav Neurosci* 2009;123:504-19.